Received: 3 October 2019 | Accepted: 27 January 2020
DOI: 10.1002/hyp.13737

WILEY

RESEARCH ARTICLE

Soil moisture temporal stability and spatio-temporal variability about a typical subalpine ecosystem in northwestern China

Xi Zhu[1] | Zhibin He[1] | Jun Du[1] | Longfei Chen[1] | Pengfei Lin[1] | Quanyan Tian[1,2]

[1]Linze Inland River Basin Research Station, Chinese Ecosystem Research Network, Key Laboratory of Eco-Hydrology of Inland River Basin, Northwest Institute of Eco-Environment and Resources, Chinese Academy of Sciences, Lanzhou, China

[2]University of Chinese Academy of Sciences, Beijing, China

Correspondence
Zhibin He, Linze Inland River Basin Research Station, Chinese Ecosystem Research Network, Key Laboratory of Eco-Hydrology of Inland River Basin, Northwest Institute of Eco-Environment and Resources, Chinese Academy of Sciences, Lanzhou 730000, China.
Email: hzbmail@lzb.ac.cn

Funding information
National Natural Science Foundation of China, Grant/Award Numbers: 41621001, 41901044; Foundation for Excellent Youth Scholars of "Northwest Institute of Eco-Environment and Resources," CAS, Grant/Award Number: FEYS2019011; The National Key Research and Development Program of China, Grant/Award Number: 2019YFC0507404

Abstract

Knowledge of the spatial–temporal variability of soil water content is critical for water management and restoration of vegetation in semi-arid areas. Using the temporal stability method, we investigated soil water relations and spatial–temporal variability of volumetric soil water content (VSWC) in the grassland–shrubland–forest transect at a typical semi-arid subalpine ecosystem in the Qilian Mountains, northwestern China. The VSWC was measured on 48 occasions to a depth of 70 cm at 50 locations along a 240-m transect during the 2016–2017 growing seasons. Results revealed that temporal variability in VSWC in the same soil layer in the three vegetation types and averaged across vegetation types tended to exhibit similar patterns of a decrease with increasing soil depth. Temporal stability in each vegetation type was stronger with an increase in soil depth. However, the results of temporal stability determined with standard deviation of relative difference (SDRD) disagreed with those based on the Spearman's rank correlation coefficient; the forest site had the highest Spearman rank correlation coefficient while the shrubland—the smallest SDRD in the 0–20 cm soil layer. Correlation analyses of VSWCs between two vegetation types indicated that soil water was related among all three vegetation types at the 0–20, and 0–70 cm soil layer, but in the 20–40 and 40–70 cm soil layers, significant correlation ($p < .01$) occurred only between adjacent vegetation types. In the upper soil layer (0–20 cm), soil water relations were mainly affected by surface runoff. In the lower soil layer (20–40 and 40–70 cm), soil water relations among the three vegetation types were highly complex, and probably resulting from a combination of root distribution and activity, interflow, and the impact of deep soil freeze–thaw dynamics. These results suggest that the factors affecting soil water are complex, and further research should address the relative importance of and interactions among different determining factors.

KEYWORDS
Qilian Mountains, soil moisture, spatio-temporal variability, temporal stability, vegetation types

1 | INTRODUCTION

Soil moisture is the principal limiting factor in water resources management, ecosystem restoration, and agricultural production in arid and semi-arid regions (del Campo, González-Sanchis, García-Prats, Ceacero, & Lull, 2019; Newman et al., 2006). As an important controlling factor of many hydrological, ecological, and biological processes, it constrains plant transpiration and photosynthesis, thereby affecting the water, energy, and biogeochemical cycles of the land surface (Babaeian et al., 2019; Brocca, Ciabatta, Massari, Camici, & Tarpanelli, 2017; Western, Grayson, Blöschl, Willgoose, & McMahon, 1999). In high mountains, soil moisture strongly influences other hydrological processes, especially horizontal fluxes, such as runoff (Grant, Seyfried, & McNamara, 2004; He, Zhao, Liu, & Tang, 2012). It is also an integrative state variable affected by climatic forcing, vegetation characteristic, soil property, and topography (Famiglietti, Ryu, Berg, Rodell, & Jackson, 2008; Majdar, Vafakhah, Sharifikia, & Ghorbani, 2018; Western et al., 1999). Spatial variability in soil moisture in different vegetation types has important implications for understanding of these eco-hydrological, and biological processes (Brocca et al., 2017; Fan et al., 2019). Therefore, analysis of soil moisture spatial–temporal variability within and among different vegetation types is important for understanding eco-hydrological processes, and for sustainable development of ecosystems in arid and semi-arid areas.

Variability in soil moisture is high. However, repeated investigations can identify particular locations which are relatively stable over time, and can represent entire study areas well (Li, Shao, Jia, & Wei, 2016). This phenomenon is known as temporal stability of soil moisture (Vachaud, Passerat de Silans, Balabanis, & Vauclin, 1985). The concept of temporal stability of soil moisture has been applied in many studies for validating and calibrating remotely sensed soil moisture data, selecting representative locations to estimate mean soil moisture content, and improving datasets containing missing data (Chen, Wen, & Tian, 2016; Dumedah & Coulibaly, 2011; Grayson & Western, 1998). It has been also broadly applied in various vegetation types, such as grassland (Zhao, Peth, Wang, Lin, & Horn, 2010), cropland (Guber et al., 2008), desert (Zhang & Shao, 2013), and forestland (He et al., 2019). In addition, temporal stability of soil moisture has been investigated at different soil depths, scales, regions, measurement periods, and measuring instruments (Dari, Morbidelli, Saltalippi, Massari, & Brocca, 2019; Fu et al., 2018; Heathman, Cosh, Merwade, & Han, 2012; Jacobs, Mohanty, Hsu, & Miller, 2004; Penna, Brocca, Borga, & Dalla Fontana, 2013). Despite these extensive efforts, it is not well known whether a temporal stability pattern and soil moisture content exist in the vegetation pattern with different vegetation types, and whether these interactions can be analysed with VSWC measured at the most time-stable locations (MTSLs) in each vegetation type.

Studies of water relations in different land use types have been conducted in many areas; Shen, Gao, Fu, and Lü (2014) pointed out that hydrological relations between tree-belt and cropland in the upper soil layer were driven by tree water uptake from cropland. They further found that hydrological relations among cropland-tree belt-desert in the lower soil layers were determined by groundwater recharge as cropland irrigation raised groundwater levels to replenish deep soil moisture. Woodall and Ward (2002) reported that tree-crop competition for reduced wheat growth and grain yield within 20–30 m of the trees. Livesley, Gregory, and Buresh (2004) also observed that soil moisture content in an alley cropping system varied spatially with distance from a tree row. These studies primarily concentrated on comparing water use of adjacent land use types and hydrological interactions between them, such as between cropland and tree-belt (Ellis, Hatton, & Nuberg, 2005; Zhang, Xiao, & Huang, 2016), or tree-belt and pasture (Knight, Blott, Portelli, & Hignett, 2002). However, little research has been done on soil water relations between different vegetation types in subalpine ecosystems. Understanding water relations between different vegetation types is of great significance to the restoration of mountain vegetation and water resource management in arid and semi-arid regions.

Combinations of land use or vegetation types had significant effects on the variability of soil moisture, especially in arid and semi-arid regions (Ruiz-Sinoga, Galeote, Murillo, & Marín, 2011; Shen et al., 2014; Valentin, d'Herbès, & Poesen, 1999). In many arid or semi-arid environments around the world landscapes frequently display a contrasting mosaic of vegetation, with high-biomass cover interspersed with a low-cover or bare soil component (Liu, Zhao, & He, 2013; Saco, Willgoose, & Hancock, 2007). In the semi-arid alpine system of the Qilian Mountains in China, topography can affect solar radiation, creating different moisture conditions and opportunities for vegetation establishment on different slope aspects. Various vegetation types (i.e., grassland, shrubland, forest) are interspersed with each other, resulting in many representative land use patterns such as grassland–forestland, shrubland–forestland, and grassland–shrubland–forestland. Previous studies on the eco-hydrological processes in this area were mainly focused on soil moisture dynamics, forest transpiration, canopy interception, and simulation of runoff (Chang et al., 2017; He et al., 2012; He et al., 2014; Zhu et al., 2017). However, spatio-temporal patterns of soil moisture and relationships with different vegetation types are still poorly understood, even though they have important implications for ecosystem management.

In this study, a grassland–shrubland–forest site in the Qilian Mountains was selected to address these issues. VSWC was measured on 48 occasions to a depth of 70 cm at 50 locations along a 240 m transect during the growing seasons in 2016 and 2017. The objectives of this study were to: (a) determine the spatial–temporal variability in VSWC within single vegetation types and across them; (b) analyse temporal stability of spatial patterns, and identify MTSLs for different soil layers in different vegetation types; and (c) investigate soil water relations between adjacent vegetation types using VSWC at the identified MTSLs (we hypothesized that soil water interactions existed between adjacent vegetation types). This study provides scientific basis for restoration of vegetation and water resources management in semi-arid mountain areas.

2 | MATERIALS AND METHODS

2.1 | Site description

The study area (centre at 38°32′N, 100°18′E, altitude 2,920 m) was located in the Pailugou catchment, which represents a typical subalpine semi-arid ecosystem, Gansu Province, northwestern China. The area has a semi-arid cold temperate climate with mean annual rainfall of 416 mm (mean value from years 1994 to 2008), and pan evaporation of 1,051.7 mm (He et al., 2014). Average annual temperature is 0.5°C with the high of 28.0°C in July, and the low of −36.0°C in January (Chang et al., 2014). The distribution of daily rainfall and mean air temperatures at the study area for study years 2016 to 2017 are shown in Figure 1.

In the study, north-facing slopes were defined as shaded, south-facing slopes were defined as sunny, southeast-facing or south by southwest-facing slopes were defined as semi-sunny, and northwest-facing slopes or northeast by north-facing slopes defined as semi-shady (Zhu et al., 2016). Grey cinnamon soil on shaded slopes, and chestnut soil on sunny slopes, are the two most common soils in the catchment. Native vegetation patterns are closely related to topographic aspects, with a mosaic of grassland, forest, and small areas of scrubland (He et al., 2012). Forests, dominated by *Picea crassifolia*, are distributed on shaded and semi-shaded, north-facing slopes. In our study area, *P. crassifolia* forest covered 38.5% of the catchment area, but contributed little (i.e., 3.5% of total annual water yield of the catchment) to annual water yield (He et al., 2012). Common species in the understory layer include shrubs such as *Potentilla fruticosa* L., *Potentilla glabra* Lodd., *Salix oritrepha* Schneid. Herbaceous species such as *Carex melanocephala* Turcz. ex Bess, *Carex atrata*, *P. fruticosa*, *Foeniculum vulgare* Mill., *Leymus chinensis* (Trin.) Tzvel, and *Polygonum viviparum* L. are mainly found on sunny, south-facing, and semi-shaded, east- or west-facing slopes. The grassland–shrubland–forest transect is north-facing, and has a relatively flat topography, with average slope of approximately 15°. And the basic descriptions of geographical, vegetation characteristics, and soil properties for our monitoring transect are shown in Table 1.

2.2 | Sampling and measurements

2.2.1 | VSWC measurements

In early July 2016, we established a 240 m long survey transect that belongs to typical subalpine ecosystems of northwestern China. Along this transect with 50 representative sampling locations at regular intervals of 5 m was established in the south–north direction across grassland, shrubland, and forest (Figure 2). A Trime-TDR tube was installed at each location for measuring VSWC. Nine (Numbered 1–9), 15 (Numbered 10–24), and 26 (Numbered 25–50) Trime-TDR tubes (special polyvinyl chloride access tubes) were installed respectively in the grassland, shrubland, and forest. For most sampling locations, VSWC can be measured to a maximum depth of 70 cm. However, VSWC data for a few sampling locations can only be obtained to a depth of 60 cm due to the presence of bedrock and permafrost below that depth.

In our study, the soil moisture data are observed manually. In order to include as many measurements as possible for each month during each measurement year, the exact measurement period for 2016 and 2017 were between 23 July 2016 and 20 November 2016, and between 22 May 2015 and 28 October 2017, respectively. Therefore, during the monitoring periods, the VSWCs at depths of 10–70 cm were measured in 10-cm depth intervals on 48 sampling occasions between 23 July 2016 and 28 October 2017 (26 sampling occasions between 23 July 2016 and 20 November 2016, and

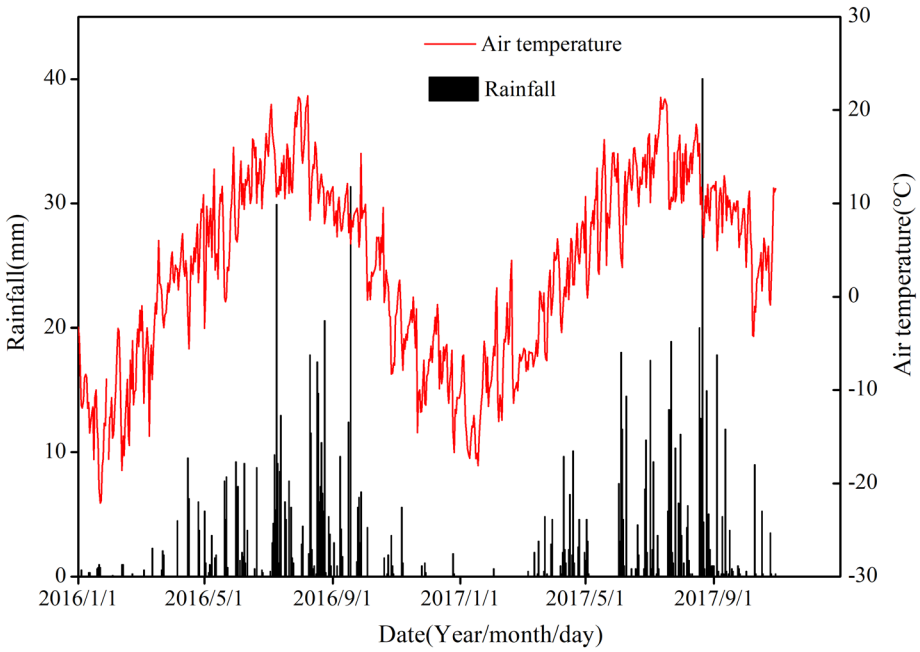

FIGURE 1 Distribution of daily rainfall and mean air temperature at the study area from 2016 to 2017

TABLE 1 Geographical, vegetation characteristics, and soil properties along the monitoring transect under different vegetation types

											Herbaceous	
Elevation (m)	Slope (°)	Aspect (°)	Vegetation types	SDE (trees/ha)	Height (m)	DBH (cm)	LAI (m^2/m^2)	SBD (g/cm^3)	Ks10 (mm/min^1)	Ks20 (mm/min^1)	TC (%)	AB (g/m^2)
2,950	15°	N	Grassland	–	–	–	–	1.03 ± 0.21a	1.53 ± 0.21a	0.89 ± 0.13a	95.5 ± 2.84a	198.58 ± 8.24a
			Shrubland	–	–	–	–	0.89 ± 0.21b	1.98 ± 0.09b	1.2 ± 0.05b	52.32 ± 3.85b	58.58 ± 5.65b
			Forest	1,800 ± 39	6.8 ± 0.89	7.4 ± 0.23	1.56 ± 0.42	0.85 ± 0.11b	2.1 ± 0.06b	1.4 ± 0.04c	48.98 ± 5.46b	47.35 ± 7.52c

Note: Values (±*SE*) followed by different lower-case letters within columns are significantly different at $p < .05$.
Abbreviations: AB, aboveground biomass; DBH, diameter at breast height; Ks10, saturated soil hydrologic conductivity at 10 cm; Ks20, saturated soil hydrologic conductivity at 20 cm; LAI, leaf area index; SBD, soil bulk density, SDE, stand density; SBD; TC, total cover.

22 occasions between 22 May 2015 and 28 October 2017). Considering the three different vegetation types along the monitoring transect, and their main root distribution depths are significantly different (e.g., the root distribution depths for herbs is mainly about 20 cm, but for shrub and forest are mainly about 30–40 cm), the following analyses were based on 48 sampling occasions under the 0–20, 20–40 and 40–70 cm soil depths.

2.2.2 | Related stand and soil properties

Three replicate sample plots of 20×20 m^2 were randomly located in each shrub and forest along the monitoring transect for a total of six sample plots. In the shrub and forest plot, tree or shrub height, diameter at breast height, leaf area index (LAI) (CI–110, CID, Inc., Washington, DC), and the number of trees or shrubs were measured. At each location, 30 cm away from the TDR-access tubes, a 20-cm deep pit was excavated for collections of undisturbed soil samples for measurements of saturated soil hydraulic conductivity (Ks mm/min^1) using the constant-head method, and of soil bulk density. We sampled peak aboveground biomass of herbs by clipping ground vegetation in an area of 1×1 m^2 at each location. Plant samples were oven-dried at 65°C to a constant weight, then weighed. Geographic coordinates, elevations, and slope angle of this transect were obtained using a global positioning system with differential correction.

2.3 | Methods

2.3.1 | Calculation of the volumetric soil water content

Volumetric soil water content (VSWC; θ) was measured using a size-matched portable probe (time domain reflectometry, TDR, IMKO, Ettlingen, Germany) at each of the 50 locations along the 240 m transect (Figure 2). The measuring accuracy between the value of the instrument and the theoretical value is 2%, and the repeatability precision for the instrument completes the corresponding results of the same change process repeatedly is 0.3%. At each location, a Trime-TDR tube (length: 100 cm; diameter: 5 cm) was installed in early 2016. Mean VSWC at depths of 10–70 cm was measured at 10-cm intervals on 48 sampling occasions during the 2016 and 2017 growing seasons. In addition, measured VSWC was calibrated in the field with the gravimetric method under both low and high soil water conditions (details in He et al. (2019)).

According to Shen et al. (2014), the mean VSWC for all locations at a given measurement time for 0–20, 20–40, and 40–70 cm layers and the entire profile (0–70 cm) was calculated as follows:

$$\bar{\theta}_{0-20,t} = \frac{1}{2n}\sum_{j=1}^{n}\sum_{i=1}^{2}\theta_{d_i,j,t}; \bar{\theta}_{20-40,t} = \frac{1}{2n}\sum_{j=1}^{n}\sum_{i=3}^{4}\theta_{d_i,j,t}; \bar{\theta}_{40-70,t} = \frac{1}{3n}\sum_{j=1}^{n}\sum_{i=5}^{7}\theta_{d_i,j,t}; \bar{\theta}_{0-70,t} = \frac{1}{7n}\sum_{j=1}^{n}\sum_{i=1}^{7}\theta_{d_i,j,t} \quad (1)$$

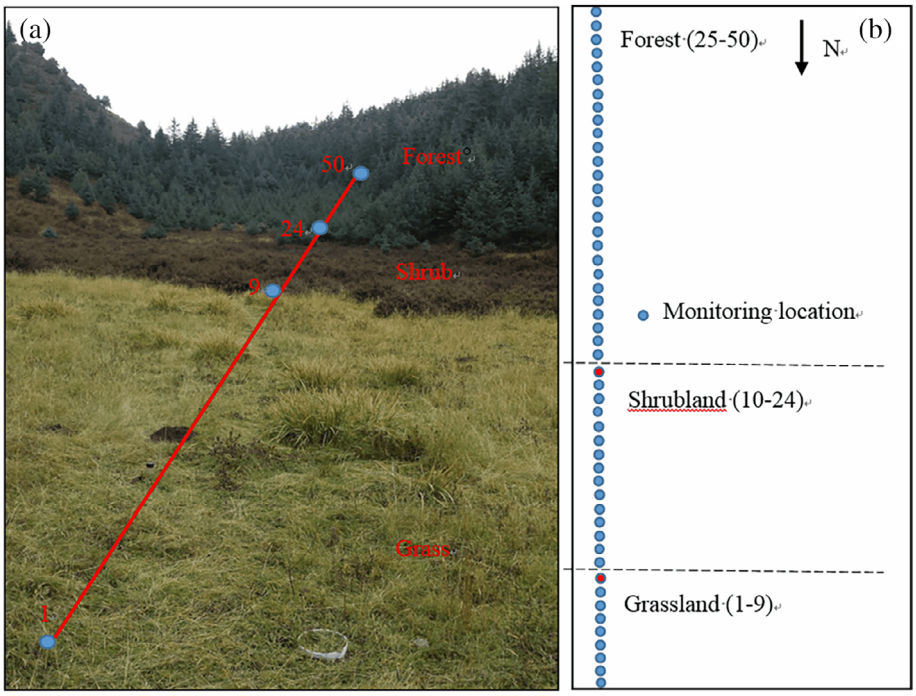

FIGURE 2 View of grassland–shrubland–forest site and schematic locations for monitoring volumetric soil water content (VSWC)

where d_i denoted the ith soil depth, j is the measurement location, and t is the measurement time. Mean VSWC of all soil layers and the entire profile (0–70 cm) during the study period for one vegetation type is calculated as follows:

$$\bar{\theta}_{0-20} = \frac{1}{T}\sum_{t=1}^{T}\bar{\theta}_{0-20,t}; \bar{\theta}_{20-40} = \frac{1}{T}\sum_{t=1}^{T}\bar{\theta}_{20-40,t}; \bar{\theta}_{40-70} = \frac{1}{T}\sum_{t=1}^{T}\bar{\theta}_{40-70,t}; \bar{\theta}_{0-70} = \frac{1}{T}\sum_{t=1}^{T}\bar{\theta}_{0-70,t} \quad (2)$$

where d_i,i, j, and t are defined as above in Equation (1), and n and T are the total number of soil water content measurement locations and occasions for one land use type, respectively.

2.3.2 | Assessment of temporal stability

The primary method was based on the relative difference, and was initially introduced by Vachaud et al. (1985). The relative difference in VSWC, δ_{ijk}, for location i, time j, and depth k is calculated as:

$$\delta_{ijk} = \frac{\mathrm{VSWC}_{ijk} - \overline{\mathrm{VSWC}}_{jk}}{\overline{\mathrm{VSWC}}_{jk}} \quad (3)$$

where $\overline{\mathrm{VSWC}}_{jk}$ is the mean SWS for transect at jth time and at kth depth:

$$\overline{\mathrm{VSWC}}_{jk} = \frac{1}{M}\sum_{i=1}^{M}\mathrm{VSWC}_{ijk} \quad (4)$$

in which M is the number of sampling locations.

The temporal mean relative difference (MRD), $\bar{\delta}_{ik}$, and the associated standard deviation of relative difference (SDRD) over time, $\sigma(\delta_{ik})$, were calculated as:

$$\bar{\delta}_{ik} = \frac{1}{N}\sum_{j=1}^{N}\delta_{ijk} \quad (5)$$

and

$$\sigma(\delta_{ik}) = \sqrt{\frac{1}{N-1}\sum_{j=1}^{N}\left(\delta_{ijk} - \bar{\delta}_{ik}\right)^2} \quad (6)$$

where N is the total number of sampling occasions. The value of MRD determined whether a location was wetter or drier than the areal mean VSWC at a particular depth, and a low SDRD indicated a high temporal stability. According to Jacobs et al. (2004) and Zhao et al. (2010), an index of temporal stability (ITS) can be computed using a combination of MRD and the associated SDRD as follows:

$$\mathrm{ITS}_{ik} = \sqrt{\bar{\delta}_{ik}^{\,2} + \sigma(\delta_{ik})^2} \quad (7)$$

The ITS provided a single metric for identifying sampling locations that were most representative of the mean plot SWS (i.e., low $\bar{\delta}_{ik}$,), and that were also temporally stable (i.e., low $\sigma(\delta_{ik})$). The location with the highest temporal stability had the lowest ITS. An acceptable ITS threshold can be established to identify sites that consistently represent mean field VSWC with accuracy (Zhao et al., 2010). In this study, sampling locations with an ITS under 10% were selected as time-stable sites.

The non-parametric Spearman's test was also used to examine the persistence of the spatial patterns over the study period (Vachaud et al., 1985). The Spearman's rank correlation coefficient (r_s) is expressed as:

$$r_s = 1 - \frac{6\sum_{i=1}^{N}\left(R_{ij} - R_{ij'}\right)^2}{n(n^2-1)} \quad (8)$$

is the rank of the same variable at the same location but at time j', and n is the number of observation locations. An r_s equal to 1 between measurement occasions indicated a strong tendency towards temporal stability.

2.3.3 | Soil water relations

In the present study, we hypothesized that soil water interactions existed between adjacent vegetation types, and that VSWC measurements made at MTSLs could be used to analyse soil water relations between adjacent vegetation types (Zhang et al., 2016).

2.4 | Statistical analysis

Exploratory data analysis was performed using Microsoft Excel. We used one-way analysis of variance (ANOVA) to test the significance of the differences in VSWC and of criteria for temporal stability among different soil depths and vegetation types; we used the least-significant-difference test when significant differences were detected by ANOVA, and significance was evaluated at the 0.05 level. Linear-fitting analysis was conducted between the measured VSWCs at the MTSLs and the mean values for each vegetation type. All statistical analyses were conducted using SPSS, version 17.0 software (SPSS Inc., Chicago, IL).

3 | RESULTS

3.1 | Soil water variability in different vegetation types

Generally, the soil moisture varied by both vegetation types and soil depths, and the VSWC tended to increase with increasing soil depth (Table 2 and Figure 3). Shrubland had the highest VSWC of the vegetation types in all three soil layers, and that was a significant difference ($p < .05$) compared with other vegetation types on the whole soil profile. In the 20–40 cm soil layer, the VSWC of shrubland was 1.1, 1.3, and 1.2 times than that of grassland, forestland, and the whole transect, respectively. On the 20–40 and 40–70 cm soil layers, the VSWC exhibited the order of shrubland, grassland, and forest. However, on the 0–20 cm soil layer, the VSWC exhibited the order of shrubland (32.95%), forest (31.66%), and grassland (25.89%) (Table 2). In addition, significant correlations ($p < .01$) were found between any two soil layers within a profile, but correlations were stronger between two adjacent layers than between two non-adjacent layers.

VSWC averaged across time in the near-surface soil layer was lower than that in deeper layers due to strong evapotranspiration; this was despite rainfall replenishment (Figure 4). The SD value was relatively high in the near-surface layer indicating high temporal variability. In contrast, temporal changes in VSWC appeared to be smaller in sub-surface and across the profile, as reflected by the decreasing SD values with increasing soil depth for all vegetation types. The vertical distribution pattern of

TABLE 2 Statistics of the VSWC for various soil layers in different vegetation types during the study period

Vegetation type	Statistics	0–20 cm	20–40 cm	40–70 cm	0–70 cm
Grassland	Mean* (%)	25.89a	38.24a	37.97c	33.51b
	Max (%)	53.21	52.81	42.96	46.49
	Min (%)	12.41	31.94	33.80	25.31
	CV** (%)	21.22	10.62	19.38	9.86
Shrubland	Mean* (%)	32.95b	41.59b	38.16c	37.07c
	Max (%)	61.39	62.77	61.58	54.70
	Min (%)	14.50	31.53	18.69	26.10
	CV** (%)	15.35	17.54	17.16	11.98
Forest	Mean* (%)	31.66b	32.01c	32.10a	31.91a
	Max (%)	45.23	44.57	51.41	46.00
	Min (%)	16.08	24.38	17.44	24.32
	CV** (%)	28.55	27.19	19.69	21.17
Grassland–shrubland–forest	Mean* (%)	31.01b	36.01d	34.97b	33.75b
	Max (%)	51.51	49.57	52.76	46.96
	Min (%)	14.95	29.37	21.15	25.03
	CV** (%)	25.39	25.11	23.27	18.55

Abbreviation: VSWC, volumetric soil water content.

*The significant differences among different land use types are indicated with different lowercase letters ($p < .05$).; **CV is the coefficient of variation.

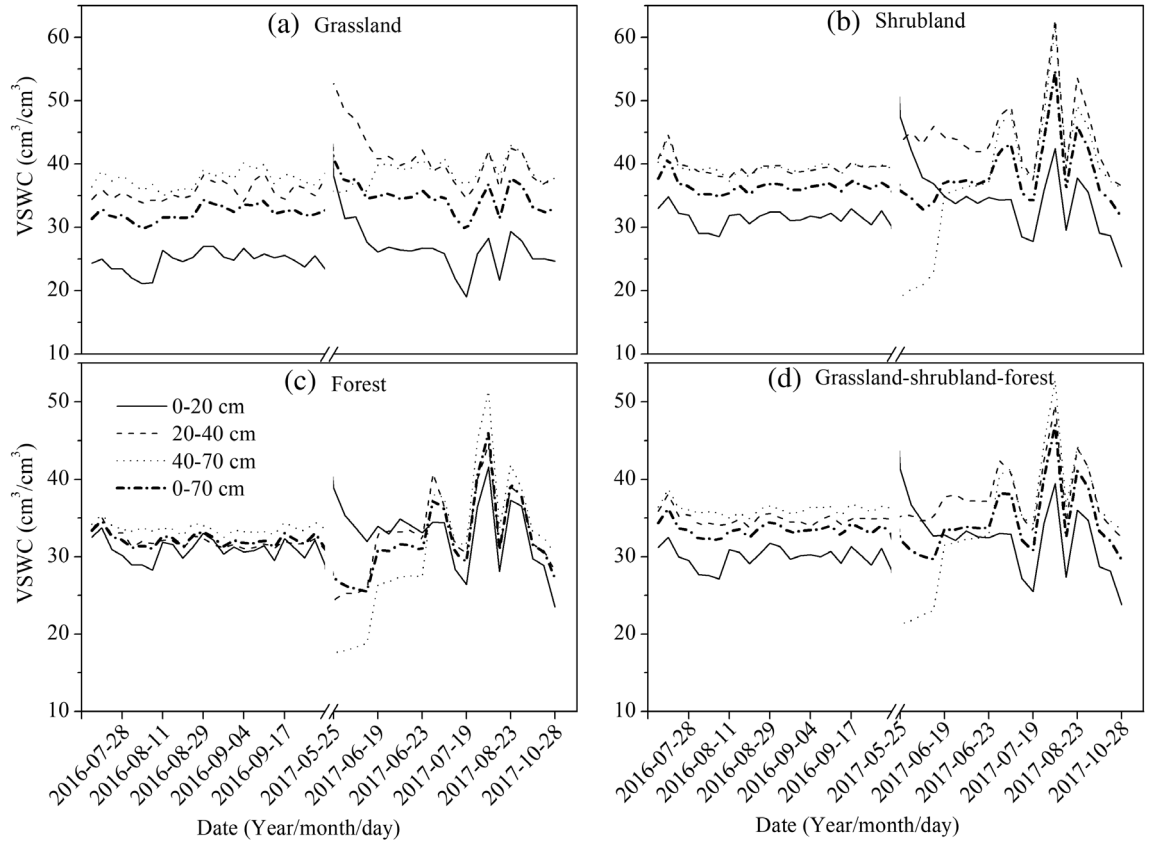

FIGURE 3 Temporal changes of the volumetric soil water content (VSWC) for various soil layers in different vegetation types

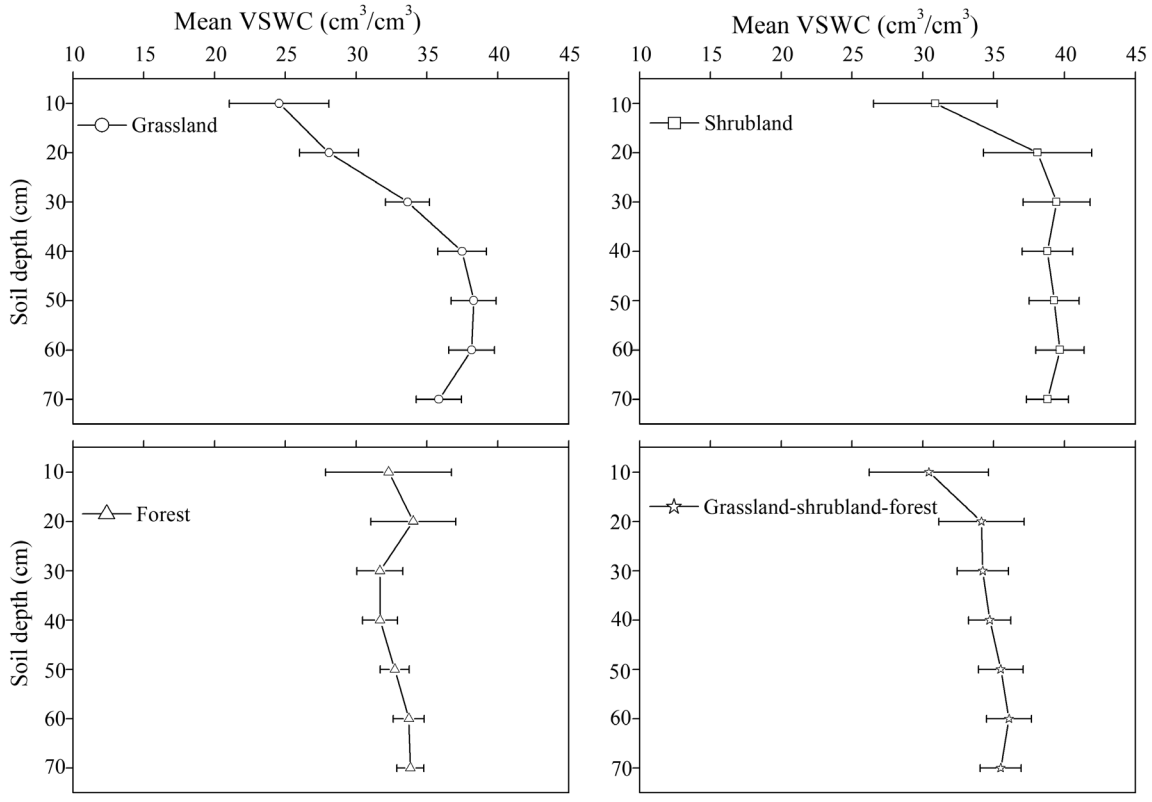

FIGURE 4 Vertical change of the mean volumetric soil water content (VSWC) under different vegetation types. Vertical bars represent 95% confidence limits. The alpha value is 2.5% at each side of the bar

TABLE 3 Summary statistics of Spearman rank correlation coefficients for different soil layers based on all measurements during the 2016–2017 study period

Vegetation type	Statistics	0–20 vs. 0–20 cm	20–40 vs. 20–40 cm	40–70 vs. 40–70 cm	0–70 vs. 0–70 cm	0–20 vs. 20–40 cm	0–20 vs. 40–70 cm	0–20 vs. 0–70 cm	20–40 vs. 40–70 cm	20–40 vs. 0–70 cm	40–70 vs. 0–70 cm
Grassland	Mean*	0.74a	0.77b	0.88c	0.89c	0.17d	−0.32e	0.41f	−0.06g	0.39f	0.41f
	Max	0.97	0.97	1.00	0.98	0.68	0.22	0.82	0.37	0.72	0.75
	Min	0.33	0.43	0.72	0.72	−0.50	−0.73	−0.12	−0.47	−0.12	0.07
	CV**	17.3%a	14.5%b	7.0%c	6.3%c	137%d	−65.5%e	52.7%f	−275%g	44.4%h	37.9%h
Shrubland	Mean*	0.76a	0.89b	0.92b	0.85b	0.14c	−0.27d	0.20c	0.48e	0.69f	0.68f
	Max	0.99	0.97	0.99	0.99	0.74	0.30	0.74	0.70	0.90	0.91
	Min	0.21	0.70	0.77	0.67	−0.14	−0.58	−0.15	0.20	0.42	0.43
	CV**	26.9%a	6.6%b	5.1%b	8.6%c	126.9%d	−58.2%e	77.5%f	22.4%a	16.1%g	14.9%g
Forest	Mean*	0.87a	0.94b	0.91b	0.93b	0.69c	0.42d	0.76e	0.64f	0.88a	0.76e
	Max	0.97	0.99	0.98	0.99	0.85	0.66	0.92	0.78	0.94	0.85
	Min	0.68	0.84	0.75	0.85	0.49	0.21	0.54	0.47	0.75	0.66
	CV**	7.7%a	3.5%b	6.1%c	3.5%b	12.55%d	23.9%e	10.5%d	9.2%f	4.8%g	5.6%g
Grassland–shurbland–forest	Mean*	0.86a	0.92b	0.91b	0.90b	0.44c	0.12d	0.59e	0.58e	0.80f	0.71f
	Max	0.96	0.98	0.97	0.97	0.64	0.31	0.77	0.67	0.90	0.90
	Min	0.70	0.83	0.84	0.78	0.23	−0.06	0.29	0.49	0.61	0.60
	CV**	8.8%a	3.5%b	3.6%b	4.9%c	22.9%d	67.1%e	16.8%f	6.5%g	6.5%g	6.9%g

*is the mean Spearman rank correlation coefficient for different soil layers based on all measurements during the 2016-2017 study period.
**is the coefficient of variation for mean Spearman rank correlation coefficient under different soil layers based on all measurements during the 2016-2017 study period.
Values followed by different lower-case letters within rows are significantly different at $P < 0.05$.

VSWC varied by vegetation type. The maximum VSWC in grassland, shrubland, forest, and whole transect were 38.2% in 50 cm depth, 39.7% in 60 cm depth, 33.8% in 70 cm depth and 36.1% in 60 cm depth, respectively. In the 0–20 cm layer, VSWC increased rapidly with depth, and the percentage increase for VSWCs in grassland, shrubland, forest, and whole transect were 14.3, 37.1, 6.1, and 13.3%, respectively. In the 40–70 cm layer, VSWC tended to increase at a relatively steady rate (the percentage increase for VSWC less 2%) under all vegetation types. However, there was a notable decline in VSWC at 30 cm in the forest site (Figure 4). VSWC at 10 cm depth exhibited the order of forest (32.28%), shrubland (30.88%), and grassland (24.56%). Shrubland had the highest VSWC at the depth of 20 cm. However, below 30 cm depth, the rank of SWS for different vegetation types was: shrubland > grassland > forest.

3.2 | Temporal stability of soil water contents for different vegetation types

3.2.1 | Temporal stability of VSWC in the soil profile

The Spearman rank correlation coefficient (r_s) matrix of different observation times in different soil layers is not shown here for the sake of brevity. In the matrix, all coefficients for each soil layer were significant at the 0.05 probability level, indicating a strong temporal stability in the four soil layers. Temporal stability, however, exhibited a time-associated drift, especially in the shallow soil layer. The r_s was significantly higher in forest than in other vegetation types. Further, the results of a one-way ANOVA showed significant differences ($p < .05$) between the 0–20 and >20 cm soil layers. However, except for grassland at 20–40 and 40–70 cm, no significant differences were found among 20–40, 40–70, and 0–70 cm soil layers for three typical vegetation types and for the average of vegetation types (Table 3). In this study, the mean Spearman rank correlation coefficients in grassland, shrubland, forest, and whole transect were 0.80, 0.86, 0.91 and 0.90, respectively (Table 3). Furthermore, the closer together and the deeper two soil layers within a given profile, the larger the Spearman rank correlation coefficient. We also found that the two soil layers only included the entire soil profile (0–70 cm), the greater the Spearman rank correlation coefficient.

3.2.2 | Temporal stability of VSWC at individual locations

The rank-ordered MRD of VSWC, the associated SDRD, and the ITS for each location for the four soil layers (Figure 5) showed that the three variables behaved differently under different vegetation types

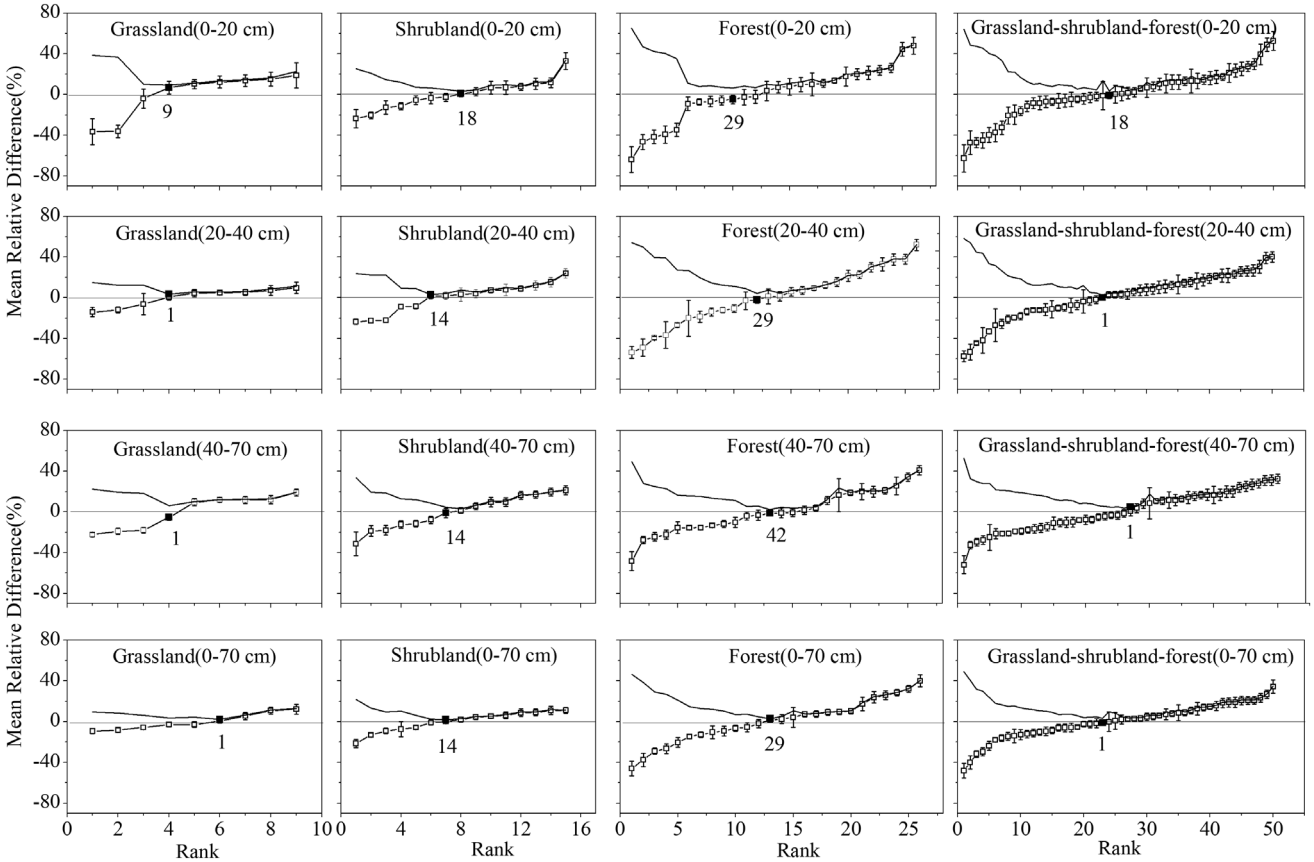

FIGURE 5 Ranked mean relative differences (MRDs) of VSWC of four soil layers under different vegetation types. Error bars represent the standard deviation of relative difference (SDRD). The most time-stable locations are indicated by the solid symbols. The curve indicates the index of time stability (ITS). Vertical bars represent 95% confidence limits. The alpha value is 2.5% at each side of the bar

(Table 4). In the whole profile (0–70 cm soil), the ranges between the minimum and maximum values for the MRD in grassland, shrubland, and forest were 19.19, 30.99, and 66.23%, respectively. In the 0–20 cm soil layer, the mean SDRD of VSWCs for grassland, shrubland, forest, and whole transect were 8.67, 8.22, 10.84 and 9.67, respectively. Which indicated that the shrubland had the greatest temporal stability in this layer, but was significantly different only between grassland and forest. In the 20–40 cm soil layer, grassland had the strongest time stability (indicated the lowest SDRD value) and that was significantly different from other vegetation types (Table 4). However, there was no significant difference in SDRD among vegetation types in the 40–70 cm soil layer. SDRD for the profile average (0–70 cm soil) was significantly different only between grassland and forest (Table 4).

Locations with minimum values of ITSs were considered to be most representative (depicted by the solid symbols in Figure 5), and could be used to estimate the average field value at long time scales. We found that the number of time-stable locations (with an ITS under 10%) generally increased with increasing soil depth under different vegetation types (Figure 5). This also indicated that the VSWC in deeper soil layers tended to be more temporally stable. Although selected representative locations changed with depth, one location can represent VSWC in different vegetation types, for the average of vegetation types below 20 cm, and for the entire soil profile (0–70 cm). To test the ability of the identified locations to accurately represent each vegetation type, the measured VSWCs at the representative locations were plotted against mean values for the four soil layers for different vegetation types (Figure 6). Linear-fitting analysis indicated that the measured VSWCs at the representative locations were significantly correlated ($p < .05$) with the calculated mean values, indicating that they can be used to estimate mean VSWC values in all of their respective soil layers under their respective vegetation type. Among vegetation types, values measured at representative locations in shrubland resulted in most accurate estimate of mean SWC in the profile as indicated by the highest R^2 values.

3.3 | Soil water relations between adjacent vegetation types

According to Section 2.3.3, the Pearson correlation was used to assess similarity in VSWC temporal patterns among vegetation types.

TABLE 4 Statistical summary of the SDRD, and MRD for VSWC in four soil layers under different vegetation types

Vegetation type	Statistical parameter	Statistics	0–20 cm	20–40 cm	40–70 cm	0–70 cm
Grassland	MRD	Max (%)	−37.31	−16.20	−19.30	−8.45
		Min (%)	17.22	10.47	15.46	10.74
		Range (%)	54.53	26.67	34.76	19.19
	SDRD	Mean* (%)	8.67ab	5.87a	15.15a	7.03a
		Max (%)	15.57	9.41	23.80	10.96
		Min (%)	5.04	3.81	6.46	4.56
Shrubland	MRD	Max (%)	−20.96	−22.73	−18.29	−19.27
		Min (%)	24.23	19.15	19.78	11.72
		Range (%)	45.19	41.88	38.07	30.99
	SDRD	Mean* (%)	8.22a	11.43b	11.51a	7.80ab
		Max (%)	12.37	21.87	21.35	12.13
		Min (%)	4.39	5.17	6.27	4.60
Forest	MRD	Max (%)	−62.47	−47.45	−33.83	−37.94
		Min (%)	45.50	38.29	24.32	28.29
		Range (%)	107.97	85.74	58.15	66.23
	SDRD	Mean* (%)	10.84b	14.98b	12.96a	10.03b
		Max (%)	19.28	30.48	23.17	20.12
		Min (%)	4.82	6.67	4.28	4.30
Grassland–shurbland–forest	MRD	Max (%)	−62.47	−47.45	−33.83	−37.94
		Min (%)	45.50	38.29	24.32	28.29
		Range (%)	107.97	85.74	58.15	66.23
	SDRD	Mean* (%)	9.67ab	12.27b	12.92a	8.82ab
		Max (%)	19.28	30.48	23.80	20.12
		Min (%)	4.39	3.81	4.28	4.30

Abbreviations: MR, mean relative difference; SDRD, standard deviation of relative difference; VSWC, volumetric soil water content.
*Mean values followed by the same letter of the columns indicate that there was no significant difference ($p < .01$) between the SDRD of a given soil layer under two different vegetation types.

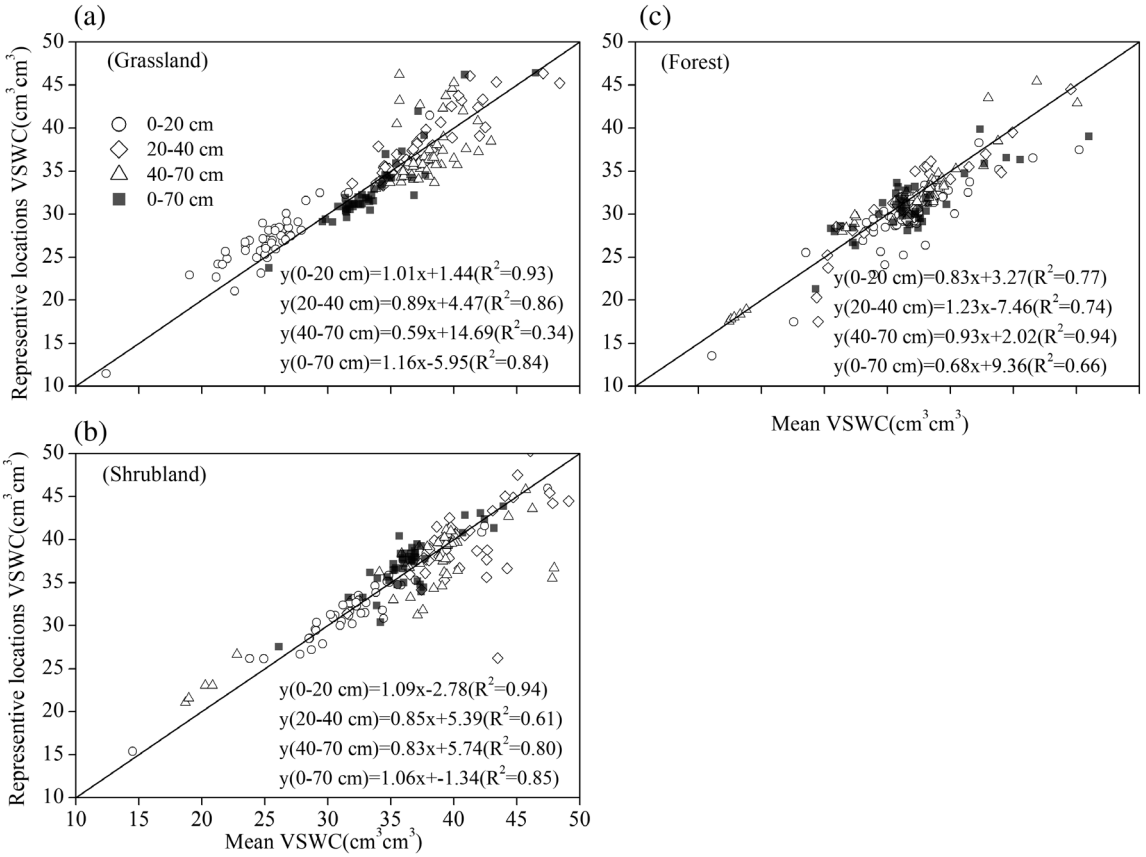

FIGURE 6 Mean VSWS vs. VSWS at the most time-stable locations (MTSLs) for different soil layers under different vegetation types. The solid line is the 1:1 line

TABLE 5 Pearson correlation coefficients between soil water contents of two vegetation types for four soil layers and entire profile. VSWC measured at the most representative sites

Soil layer (cm)	Pearson correlation coefficient		
	Grassland and shrubland	Forest and shrubland	Forest and grassland
0–20	0.89[a]	0.93[a]	0.92[a]
20–40	0.38	0.68[a]	0.19
40–70	0.41[b]	0.28	0.27
0–70	0.85[a]	0.62[a]	0.59[a]

[a]Significance level less than 0.01.
[b]Significance level less than 0.05.

Temporal patterns in VSWC distribution in the 0–20 cm soil layer and in the 0–70 cm profile in different vegetation-type combinations were significantly correlated ($p < .01$) (Table 5). However, the Pearson correlation coefficients in the 0–20 cm soil layer were lower than that of in the 0–70 cm profile. For example, the Pearson correlation coefficients between 0–20 and 0–70 cm for grassland and shrubland, forest and shrubland, and forest and grassland were 0.89, 0.93, 0.92, and 0.85, 0.62, 0.59, respectively. Significant correlations ($p < .01$) in the 20–40 and 40–70 cm soil layers occurred only between adjacent vegetation types, and no significant correlations ($p < .01$) were found between grassland and shrubland, and between forest and shrubland at those depths (Table 5). These findings indicated that VSWC measured at MTSLs can be used to investigate soil water relations between adjacent vegetation types at certain soil depths only.

The correlation coefficients relating VSWC values between adjacent vegetation types at different distances from their common borders (shrubland) are presented in Table 6. Soil water relations between adjacent vegetation types were affected by both the distance from the common boundary between vegetation types to the measurement point, and the depth of the soil layer. In the 0–20 cm soil layer and 0–70 cm soil profile, soil water was significantly correlated across locations ($p < .01$). In contrast, significant soil water relations occurred only among neighbouring locations (e.g., Distance from the bottom edge of the shrubland were 7.5 and 12.5 m in grassland locations; but distance from the top edge of the shrubland were 2.5, 7.5 and 12.5 m in forestland locations) in adjacent vegetation types in the 20–40 and 40–70 cm (deeper) soil layers. In the 20–40 cm soil layer, soil water relations were stronger between forest and shrubland than between shrubland and grassland, as indicated by higher respective correlation coefficients; opposite results were found in the 40–70 cm soil layer.

TABLE 6 Correlation coefficient matrix of soil water contents of the four soil layers at different distances from the border between adjacent vegetation types

	Distance from the bottom edge of the shrubland	Location in grassland			Distance from the top edge of the shrubland	Location in forest		
		2.5 (9)	7.5 (8)	12.5 (7)		2.5 (25)	7.5 (26)	12.5 (27)
0–20 cm layer								
Location in shrubland	2.5 (10)	0.69[a]	0.74[a]	0.69[a]	2.5 (24)	0.81[a]	0.76[a]	0.77[a]
	7.5 (11)	0.91[a]	0.57[a]	0.92[a]	7.5 (23)	0.79[a]	0.93[a]	0.89[a]
	12.5 (12)	0.88[a]	0.43[a]	0.87[a]	12.5 (22)	0.90[a]	0.81[a]	0.75[a]
20–40 cm layer								
Location in shrubland	2.5 (10)	0.27	0.74[a]	0.41[b]	2.5 (24)	0.54[a]	0.45[b]	0.55[b]
	7.5 (11)	0.17	0.39[b]	0.40[b]	7.5 (23)	0.75[a]	0.51[b]	0.55[a]
	12.5 (12)	0.20	0.60[a]	0.62[a]	12.5 (22)	0.48[b]	0.52[a]	0.72[a]
40–70 cm layer								
Location in shrubland	2.5 (10)	0.36	0.51[a]	0.45[b]	2.5 (24)	0.55[a]	0.45[b]	0.54[a]
	7.5 (11)	0.38	0.33	0.42[b]	7.5 (23)	0.39[b]	−0.22	0.17
	12.5 (12)	0.61[a]	0.60[a]	0.48[b]	12.5 (22)	0.45[b]	0.57[a]	0.34
0–70 cm layer								
Location in shrubland	2.5 (10)	0.55[a]	0.72[a]	0.61[a]	2.5 (24)	0.76[a]	0.81[a]	0.76[a]
	7.5 (11)	0.69[a]	0.71[a]	0.77[a]	7.5 (23)	0.74[a]	0.60[a]	0.68[a]
	12.5 (12)	0.69[a]	0.70[a]	0.79[a]	12.5 (22)	0.90[a]	0.89[a]	0.80[a]

Abbreviation: VSWC, volumetric soil water content.
[a]Significance level less than 0.01.
[b]Significance level less than 0.05.

4 | DISCUSSION

4.1 | Soil water content variability in different vegetation types

Different vegetation patterns can lead to significant variability in eco-hydrological dynamics due to the fundamental role plants play in controlling surface energy and water balance (Gutiérrez-Jurado, Vivoni, Harrison, & Guan, 2006). One of the most important effects of vegetation on eco-hydrological processes is soil moisture. Vegetation impacts on soil moisture dynamics include effects on rainwater inputs due to interception and stem-flow (He et al., 2014; Molina et al., 2019), soil surface temperature due to plant shading (Breshears, Nyhan, Heil, & Wilcox, 1998), soil moisture availability due to plant root water extraction (Shrestha et al., 2018), soil infiltration capacity due to vegetation patches and root channels (Wilcox, Breshears, & Turin, 2003), plant contribution to evapotranspiration (Chang et al., 2014), and deep vadose zone percolation (Fan, Baumgartl, Scheuermann, & Lockington, 2015). In this study, VSWC in the soil profile (0–70 cm) under each vegetation type differed significantly among vegetation types in the order: shrubland > grassland > forest (Table 2); this may be due to the combined effects of the above factors, and in that, our findings partially confirmed the results of previous studies.

Surface soil moisture in semi-arid areas is more prone to be affected by rainfall, vegetation transpiration, and soil evaporation than that in wetter environments (Jiao et al., 2017; Seneviratne et al., 2010; Teuling & Troch, 2005). Relatively low surface soil moisture is expected due to high evapotranspiration in semi-arid regions. In this study, grassland exhibited the lowest VSWC of all vegetation types in surface soil (0–20 cm). This was somewhat consistent with findings in other study areas (Mishra & Singh, 2010; Yang, Wei, Chen, Chen, & Wang, 2014). Although shrubland and forest had relatively high canopy interception due to high leaf area indices, the effects of plant shading can decrease radiation levels to soil and surface soil evaporation (Hasselquist, Benegas, Roupsard, Malmer, & Ilstedt, 2018; Wang, Shao, Zhu, & Liu, 2011). In addition, understory vegetation in forest and shrubland was mainly composed of mosses (data not shown), known for their excellent water retention (Michel, Lee, During, & Cornelissen, 2012). Further, even though surface VSWC in shrubland was highest in this study, it did not significantly differ from that in the forest. This was likely due to sparser grassland canopy allowing increased radiation levels to enhance soil evaporation, and to promote photosynthesis and the growth of grass, all of which can accelerate the depletion of soil moisture (Feng, Qiu, & Zhang, 2014; Raz-Yaseef, Rotenberg, & Yakir, 2010). In addition, although canopy interception in shrubland was about 2% higher than that of forest (mean of 37.0% (Ma et al., 2017) and 35.1% (He et al., 2014), respectively), the closed shrub canopy may benefit soil water retention resulting in higher VSWC in shrubland.

Root-zone soil moisture is an important water source for vegetation development in arid and semi-arid regions (Chen, Shao, & Li,

2008; Fu, Huang, Gallichand, & Shao, 2012; Nan, Wang, Jiao, Zhu, & Sun, 2019). In this study, the time-averaged mean VSWC in the 20–40 cm soil layer differed significantly across vegetation types, with highest values in shrubland (Figure 4 and Table 2). These results can be attributed to differences in the distribution of plants roots, recharge by rainfall, and specifically, to the more pronounced evapotranspiration of plants, and soil freezing and thawing in this layer. We also found that VSWCs in all vegetation types increased with soil depth, but there was a notable decline at 30 cm depth in the forest site (Figure 4). This was most likely due to the root biomass of *P. crassifolia*, found mainly at about 30 cm soil depth, which consumed excessive amounts of soil moisture stored in this layer. Previous studies also showed that soil moisture was lower in the root zone due to water consumption by roots and a presence of large pores increasing soil infiltration or drainage (Fan et al., 2015; Nan et al., 2019; Shrestha et al., 2018). Generally, soil moisture below 40 cm could be affected by plant root systems (February & Higgins, 2010), resulting in a dry zone. However, we found that VSWC at 20–40 cm in grassland and shrubland, but not in forestland, was significantly higher than that in other layers (Table 2). Root biomass in forest and in shrubland in the 20–40 cm soil layer was relatively high, but had large rainfall (>20 mm) infiltration recharge (He et al., 2012) resulted in larger VSWCs. This may also explain relatively high soil moisture in the subsurface (~40 cm) layers; similar results were reported by other researchers (Weltzin & McPherson, 1997; Yang et al., 2014; Yu et al., 2018).

4.2 | Spatial and temporal stability of soil water in different vegetation types

In this study, spatial variability in VSWC could be described by the range of MRD. MRD of the different vegetation types decreased with increasing soil depth (Table 4). The decreasing ranges of MRD may be due to the weakening spatial variability in VSWC with increasing soil depth; our findings were consistent with those observed in studies with both smaller and larger scales of sampling (Huang et al., 2018; Jia, Shao, Wei, & Wang, 2013; Martínez-Fernández & Ceballos, 2003). The range of MRD in the forest was the largest of the vegetation types used in this study, and this may indicate higher spatial and temporal variability in forestland. However, the summary statistics of r_s for different soil layers under different vegetation types indicated that forestland had the strongest temporal stability of all vegetation types (Table 3). These differences may be attributed to the different concepts of temporal stability represented by r_s and SDRD; namely, r_s is used to describe the similarity of spatial patterns in VSWC at different times, while SDRD is used to characterize the degree of temporal stability at a certain location (Gao & Shao, 2012). However, uneven plant cover, canopy interception, and the distribution of plant roots may cause a highly dynamic plant water demand and complicate such correlations (Zhao et al., 2010). Similar results were also found in other areas (Brocca, Melone, Moramarco, & Morbidelli, 2009; Duan, Huang, Li, Zhang, & Zhang, 2017; Gao & Shao, 2012; Vachaud et al., 1985).

Many studies focused on the relationship between temporal patterns of soil moisture and soil depth within a wide variety of ecosystems (Gao & Shao, 2012; Grant et al., 2004; He et al., 2019; Huang et al., 2018; Lin, 2006; Liu et al., 2018). Although we found lower mean r_s than those above reported studies, we also found a significant increase in stability with soil depth. In addition, we also found that the temporal stability exhibited a time-associated drift, especially in the shallow soil layer. These may be attributed to the following two reasons: First, due to the relatively small water uptake by vegetation, variations derived from topography or vegetations, and the ability to retain water under the deep soil layers, the stability of the soil water were increased with increasing soil depth (Kamgar, Hopmans, Wallender, & Wendroth, 1993; Korsunskaya, Gummatov, & Pachepskiy, 1995). Second, the strong heterogeneity of canopy interception (i.e., ranging from −8.77 to 84.05% in *P. crassifolia* forest as reported by He et al. (2014), and from 29.7 to 44.3% in a typical shrubland as reported by Ma et al. (2017)) and of distribution of root biomass in the study area introduced more variability in VSWC in the rooting zone (~40 cm depth), and thus decreased temporal stability in the shallow soil layer.

Generally, mean values of SDRD decreased with increasing soil depth (Hu, Shao, & Reichardt, 2010; Jia et al., 2013; Zhang et al., 2016). However, in this study, mean values of SDRD generally increased with increasing soil depth in all vegetation types except in grassland (Table 4). Besides the dissimilar soil moisture, root biomass, and the distinctive freezing and thawing dynamics at different soil depths for different vegetation types. It is mainly due to the grassland is at the bottom of the sample transect slope, which is more susceptible to the combine effects of the above factors. Except for the 0–20 cm soil layer, we also found that a single time-stable location can be used to estimate mean VSWC well, with a relative precision of <0.05 for different soil layers (Figure 6). These results were consistent with other studies, which they found that a single location can represent mean soil water content for all soil layers (Duan et al., 2017; Jia et al., 2013; Penna et al., 2013). Although least accurate estimations (R^2 = .34) of VSWC were obtained for the 40–70 cm depth in grassland, but these above findings suggested that the representative locations were appropriate for estimating (R^2 > .61, p < .05) mean VSWC at various depths at the transect scale. However, the R^2 values in our study were lower (mean R^2 = .97) than that of a grassland in the Liudaogou watershed of the Loess Plateau, China (Jia et al., 2013). Therefore, we demonstrated the feasibility of representing mean VSWC directly by measuring soil moisture at a time-stable location on a transect scale.

4.3 | Soil water relations in adjacent vegetation types

Spatial–temporal variability and soil water relations that occur within and among different vegetation types play an important role in eco-hydrological processes and sustainable development of ecosystems in arid and semi-arid areas (del Campo et al., 2019). In addition to the

confluence of slope, the characteristics of plant canopies, distribution of plants roots, and soil freezing and thawing processes affected soil water relations between adjacent vegetation types (Ellis et al., 2005; Grant et al., 2004; Qin et al., 2017; Starkloff, Stolte, Hessel, Ritsema, & Jetten, 2018; Williams, McNamara, & Chandler, 2009; Zhang et al., 2016). We found that temporal patterns of VSWC in 0–20 cm soil layer and 0–70 cm soil profile were significantly correlated ($p < .01$) among all three vegetation types (Table 5). This may be mainly due to the combined effects of snow characteristics, soil freezing, and thawing processes. In our study site, the period of snow melt mainly occurred from October to April of the following year, and the snowfall amount (mm), snow cover thickness (cm), snow density (g/cm^3), and the snow melting rate ($mm.d^{-1}$) were 4.01, 10.2, 0.25, and 1.65, respectively (Li, Li, Liu, Wang, & Zhao, 2017; Wang et al., 2011). During our monitoring periods, some measurement occasions (13 October, 04 November, and 20 November in 2016; 28 October, 2017) are included in the period of snow melt, thus the soil water relations between two adjacent vegetation types maybe due to the reason of snow melt. In addition, the seasonal frozen soil is widely existed in the study area. The time when frozen soil begins to freeze was about October 25 of the previous year, which begins to melt about March 30 of the next year, and melts completely around June 15 of the next year (Wang, Jiang, & Jing, 2017). Further, correlation occurred only between adjacent vegetation types, but not between grassland and shrubland in the 20–40 cm soil layer, or between forest and shrubland in the 40–70 cm soil layer (Table 5). This may be mainly due to the differences in plant canopies and distribution of root biomass. The soil profile in our study site was relatively shallow (mean depth of about 60 ± 10 cm), and root biomass was mainly distributed to 40 cm soil depth. In addition, high heterogeneity of plant canopy interception rate (He et al., 2014; Ma et al., 2017) in the study area also introduced more variability in VSWC in the rooting zone (~40 cm depth), and increased the complexity of the soil relations between vegetation types.

Soil water relations between adjacent vegetation types were affected by both, the distance from the border and the depth of the soil layer. In the 0–20 cm soil layer and 0–70 cm soil profile, soil water was significantly related among sampling locations regardless of distance from the border to adjacent vegetation type ($p < .01$). However, Shen et al. (2014) found that soil water in a cropland at 0–160 cm depth decreased faster closer to an adjacent tree-belt, and that the amount of loss of soil water storage was higher in sampling locations near the tree-belt than further away in the cropland; similar trends were reported in a hedge-maize system (Rosecrance, Brewbaker, & Fownes, 1992) and grevillea-maize system (Livesley et al., 2004). Our results were not consistent with those of previous studies, and that may indicate that the soil water relations in our study were mainly affected by soil freezing and thawing processes; these processes "outcompeted" the influence of plant canopies, and those of the distribution of plants roots in these soil layers. This may also explain the significant soil water relation among themselves in the 0–20 and 0–70 cm soil layers.

In contrast, significant soil water relations only occurred among close locations between adjacent vegetation types in the 20–40 and 40–70 cm soil layers. Soil water relations in the 20–40 cm soil layer were stronger between forest and shrubland than between shrubland and grassland, but the opposite was true in the 40–70 cm soil (Table 6). In addition to the relatively shallow soil layer (the mean soil depth about 60 cm) in the study site, this may be due to the strong root activity of forests and shrubs in the 20–40 cm layer. However, root activity of shrubs and grasses in the 40–70 cm layer was relatively small, and the soil water relations between shrubland and grassland were probably mainly affected by the freeze–thaw processes. Other researchers found that water relations between different land uses were affected by the distance from their common borders, and by root depth, precipitation, irrigation, and other management measures (Ellis et al., 2005; Knight et al., 2002; Malik & Sharma, 1990; Zhang et al., 2016). These indicate that the factors affecting soil water relations among different vegetation types are complex, and involve a combination of root distribution and activity, interflow, and the impact of deep soil freezing and thawing. Therefore, an adequate understanding of factors (both the relative importance of, and their interactions) influencing soil water relations in different vegetation types is critical for sustainable development in these areas.

5 | CONCLUSIONS

We investigated soil water relations and spatial–temporal variability in VSWC in 0–70 cm soil profiles in a grassland–shrubland–forest transect in a typical subalpine semi-arid ecosystem in the Qilian Mountains of China. Results revealed that the rank of average VSWC in 0–70 cm soil in different vegetation types was: shrubland > grassland > forest, but the difference between grassland and forest was not significant. Temporal stability of VSWC in each vegetation type was stronger with an increase in soil depth, and the closer two soil layers were within a given profile, and the deeper any two adjacent soil layers were, the more similar the temporal pattern of VSWC. Except for 40–70 cm in the grassland, VSWC measured at representative locations can accurately estimate ($R^2 > .61$, $p < .05$) the mean VSWS for the four soil layers under different vegetation types. Correlation analyses between VSWCs measured at representative locations in two vegetation types indicated that soil water in the 0–20, and 0–70 cm soil layer was related among the three vegetation types. However, in the 20–40 and 40–70 cm soil layers, significant correlation ($p < .01$) occurred only between adjacent vegetation types. These results indicate that the factors affecting soil water relations among different vegetation types are complex, and may include a combination of root distribution and activity, interflow, and the impact of deep soil freezing and thawing.

ACKNOWLEDGEMENTS

This work was supported by the National Key Research and Development Program of China (2019YFC0507404), Funds for National Natural Science Foundation of China (Nos. 41621001 and 41901044), and Foundation for Excellent Youth Scholars of Northwest Institute of Eco-Environment and Resources, CAS (FEYS2019011).

ORCID

Xi Zhu https://orcid.org/0000-0001-9259-1490

Pengfei Lin https://orcid.org/0000-0002-9798-8670

REFERENCES

Babaeian, E., Sadeghi, M., Jones, S. B., Montzka, C., Vereecken, H., & Tuller, M. (2019). Ground, proximal, and satellite remote sensing of soil moisture. *Reviews of Geophysics*, *57*(2), 530–616. https://doi.org/10.1029/2018RG000618

Breshears, D. D., Nyhan, J. W., Heil, C. E., & Wilcox, B. P. (1998). Effects of woody plants on microclimate in a semiarid woodland: Soil temperature and evaporation in canopy and intercanopy patches. *International Journal of Plant Sciences*, *159*(6), 1010–1017. https://doi.org/10.1086/314083

Brocca, L., Ciabatta, L., Massari, C., Camici, S., & Tarpanelli, A. (2017). Soil moisture for hydrological applications: Open questions and new opportunities. *Water*, *9*(2), 140. https://doi.org/10.3390/w9020140

Brocca, L., Melone, F., Moramarco, T., & Morbidelli, R. (2009). Soil moisture temporal stability over experimental areas in Central Italy. *Geoderma*, *148*(3–4), 364–374. https://doi.org/10.1016/j.geoderma.2008.11.004

Chang, X., Zhao, W., Liu, B., Liu, H., He, Z., & Du, J. (2017). Can forest water yields be increased with increased precipitation in a Qinghai spruce forest in arid northwestern China? *Agricultural and Forest Meteorology*, *247*, 139–150. https://doi.org/10.1016/j.agrformet.2017.07.019

Chang, X., Zhao, W., Liu, H., Wei, X., Liu, B., & He, Z. (2014). Qinghai spruce (*Picea crassifolia*) forest transpiration and canopy conductance in the upper Heihe River Basin of arid northwestern China. *Agricultural and Forest Meteorology*, *198*, 209–220. https://doi.org/10.1016/j.agrformet.2014.08.015

Chen, H., Shao, M., & Li, Y. (2008). Soil desiccation in the Loess Plateau of China. *Geoderma*, *143*(1–2), 91–100. https://doi.org/10.1016/j.geoderma.2007.10.013

Chen, J., Wen, J., & Tian, H. (2016). Representativeness of the ground observational sites and up-scaling of the point soil moisture measurements. *Journal of Hydrology*, *533*, 62–73. https://doi.org/10.1016/j.jhydrol.2015.11.032

Dari, J., Morbidelli, R., Saltalippi, C., Massari, C., & Brocca, L. (2019). Spatial-temporal variability of soil moisture: Addressing the monitoring at the catchment scale. *Journal of Hydrology*, *570*, 436–444. https://doi.org/10.1016/j.jhydrol.2019.01.014

del Campo, A. D., González-Sanchis, M., García-Prats, A., Ceacero, C. J., & Lull, C. (2019). The impact of adaptive forest management on water fluxes and growth dynamics in a water-limited low-biomass oak coppice. *Agricultural and Forest Meteorology*, *264*, 266–282. https://doi.org/10.1016/j.agrformet.2018.10.016

Duan, L., Huang, M., Li, Z., Zhang, Z., & Zhang, L. (2017). Estimation of spatial mean soil water storage using temporal stability at the hillslope scale in black locust (*Robinia pseudoacacia*) stands. *Catena*, *156*, 51–61. https://doi.org/10.1016/j.catena.2017.03.023

Dumedah, G., & Coulibaly, P. (2011). Evaluation of statistical methods for infilling missing values in high-resolution soil moisture data. *Journal of Hydrology*, *400*(1–2), 95–102. https://doi.org/10.1016/j.jhydrol.2011.01.028

Ellis, T., Hatton, T., & Nuberg, I. (2005). An ecological optimality approach for predicting deep drainage from tree belts of alley farms in water-limited environments. *Agricultural Water Management*, *75*(2), 92–116. https://doi.org/10.1016/j.agwat.2004.12.004

Famiglietti, J. S., Ryu, D., Berg, A. A., Rodell, M., & Jackson, T. J. (2008). Field observations of soil moisture variability across scales. *Water Resources Research*, *44*(1), W01423. https://doi.org/10.1029/2006WR005804

Fan, J., Baumgartl, T., Scheuermann, A., & Lockington, D. A. (2015). Modeling effects of canopy and roots on soil moisture and deep drainage. *Vadose Zone Journal*, *14*(2), 1–18. https://doi.org/10.2136/vzj2014.09.0131

Fan, Y., Clark, M., Lawrence, D. M., Swenson, S., Band, L. E., Brantley, S. L., … Kirchner, J. W. (2019). Hillslope hydrology in global change research and earth system modeling. *Water Resources Research*, *55*(2), 1737–1772. https://doi.org/10.1029/2018WR023903

February, E. C., & Higgins, S. I. (2010). The distribution of tree and grass roots in savannas in relation to soil nitrogen and water. *South African Journal of Botany*, *76*(3), 517–523. https://doi.org/10.1016/j.sajb.2010.04.001

Feng, Y., Qiu, G. Y., & Zhang, Q. (2014). Determination of canopy-shadow-affected area in sparse steppes and its effects on evaporation and evapotranspiration. *Ecohydrology*, *7*(6), 1589–1603. https://doi.org/10.1002/eco.1482

Fu, W., Huang, M., Gallichand, J., & Shao, M. (2012). Optimization of plant coverage in relation to water balance in the Loess Plateau of China. *Geoderma*, *173*, 134–144. https://doi.org/10.1016/j.geoderma.2011.12.016

Fu, Z., Wang, Y., An, Z., Hu, W., Mostofa, K. M., Li, X., & Liu, B. (2018). Spatial and temporal variability of 0-to 5-m soil–water storage at the watershed scale. *Hydrological Processes*, *32*(16), 2557–2569. https://doi.org/10.1002/hyp.13172

Gao, L., & Shao, M. (2012). Temporal stability of soil water storage in diverse soil layers. *Catena*, *95*, 24–32. https://doi.org/10.1016/j.catena.2012.02.020

Grant, L., Seyfried, M., & McNamara, J. (2004). Spatial variation and temporal stability of soil water in a snow-dominated, mountain catchment. *Hydrological Processes*, *18*(18), 3493–3511. https://doi.org/10.1002/hyp.5798

Grayson, R. B., & Western, A. W. (1998). Towards areal estimation of soil water content from point measurements: Time and space stability of mean response. *Journal of Hydrology*, *207*(1–2), 68–82. https://doi.org/10.1016/S0022-1694(98)00096-1

Guber, A. K., Gish, T. J., Pachepsky, Y. A., van Genuchten, M. T., Daughtry, C. S. T., Nicholson,T. J., & Cady, R. E. (2008). Temporal stability in soil water content patterns across agricultural fields. *Catena*, *73*(1), 125–133. https://doi.org/10.1016/j.catena.2007.09.010

Gutiérrez-Jurado, H. A., Vivoni, E. R., Harrison, J. B. J., & Guan, H. (2006). Ecohydrology of root zone water fluxes and soil development in complex semiarid rangelands. *Hydrological Processes: An International Journal*, *20*(15), 3289–3316. https://doi.org/10.1002/hyp.6333

Hasselquist, N. J., Benegas, L., Roupsard, O., Malmer, A., & Ilstedt, U. (2018). Canopy cover effects on local soil water dynamics in a tropical agroforestry system: Evaporation drives soil water isotopic enrichment. *Hydrological Processes*, *32*(8), 994–1004. https://doi.org/10.1002/hyp.11482

He, Z. B., Yang, J. J., Du, J., Zhao, W. Z., Liu, H., & Chang, X. X. (2014). Spatial variability of canopy interception in a spruce forest of the semiarid mountain regions of China. *Agricultural and Forest Meteorology*, *188*, 58–63. https://doi.org/10.1016/j.agrformet.2013.12.008

He, Z. B., Zhao, M. M., Zhu, X., Du, J., Chen, L. F., Lin, P. F., & Li, J. (2019). Temporal stability of soil water storage in multiple soil layers in high-elevation forests. *Journal of Hydrology*, *569*, 532–545. https://doi.org/10.1016/j.jhydrol.2018.12.024

He, Z. B., Zhao, W. Z., Liu, H., & Tang, Z. X. (2012). Effect of forest on annual water yield in the mountains of an arid inland river basin: A case study in the Pailugou catchment on northwestern China's Qilian Mountains. *Hydrological Processes*, *26*(4), 613–621. https://doi.org/10.1002/hyp.8162

Heathman, G. C., Cosh, M. H., Merwade, V., & Han, E. (2012). Multi-scale temporal stability analysis of surface and subsurface soil moisture within the upper Cedar Creek watershed, Indiana. *Catena*, *95*, 91–103. https://doi.org/10.1016/j.catena.2012.03.008

Hu, W., Shao, M., & Reichardt, K. (2010). Using a new criterion to identify sites for mean soil water storage evaluation. *Soil Science Society of*

America Journal, *74*(3), 762–773. https://doi.org/10.2136/sssaj2009.0235

Huang, Z., Miao, H. T., Liu, Y., Tian, F. P., He, H., Shen, W., … Wu, G. L. (2018). Soil water content and temporal stability in an arid area with natural and planted grasslands. *Hydrological Processes*, *32*(25), 3784–3792. https://doi.org/10.1002/hyp.13289

Jacobs, J. M., Mohanty, B. P., Hsu, E. C., & Miller, D. (2004). SMEX02: Field scale variability, time stability and similarity of soil moisture. *Remote Sensing of Environment*, *92*(4), 436–446. https://doi.org/10.1016/j.rse.2004.02.017

Jia, X., Shao, M. A., Wei, X., & Wang, Y. (2013). Hillslope scale temporal stability of soil water storage in diverse soil layers. *Journal of Hydrology*, *498*, 254–264. https://doi.org/10.1016/j.jhydrol.2013.05.042

Jiao, Y., Lei, H., Yang, D., Huang, M., Liu, D., & Yuan, X. (2017). Impact of vegetation dynamics on hydrological processes in a semi-arid basin by using a land surface-hydrology coupled model. *Journal of Hydrology*, *551*, 116–131. https://doi.org/10.1016/j.jhydrol.2017.05.060

Kamgar, A., Hopmans, J. W., Wallender, W. W., & Wendroth, O. (1993). Plotsize and sample number for neutron probe measurements in small field trials. *Soil Science*, *156*(4), 213–224.

Knight, A., Blott, K., Portelli, M., & Hignett, C. (2002). Use of tree and shrub belts to control leakage in three dryland cropping environments. *Australian Journal of Agricultural Research*, *53*(5), 571–586. https://doi.org/10.1071/AR01089

Korsunskaya, L. P., Gummatov, N. G., & Pachepskiy, Y. A. (1995). Seasonal changes in root biomass, carbohydrate content, and structural characteristics of gray forest soil. *Eurasian Soil Science*, *27*(9), 45–52.

Li, H. S., Li, G., Liu, X. D., Wang, S. L., & Zhao, Y. H. (2017). Snowmelt processes in *Picea crassifolia* forest land at different elevations in Qilian Mountains. *Journal of Northwest Forestry University*, *32*(4), 1–6 (in Chinese with English abstract).

Li, X., Shao, M. A., Jia, X., & Wei, X. (2016). Profile distribution of soil–water content and its temporal stability along a 1340-m long transect on the Loess Plateau, China. *Catena*, *137*, 77–86. https://doi.org/10.1016/j.catena.2015.09.005

Lin, H. (2006). Temporal stability of soil moisture spatial pattern and subsurface preferential flow pathways in the Shale Hills catchment. *Vadose Zone Journal*, *5*(1), 317–340. https://doi.org/10.2136/vzj2005.0058

Liu, H., Zhao, W., & He, Z. (2013). Self-organized vegetation patterning effects on surface soil hydraulic conductivity: A case study in the Qilian Mountains, China. *Geoderma*, *192*, 362–367. https://doi.org/10.1016/j.geoderma.2012.08.008

Liu, Z., Wang, Y., Yu, P., Tian, A., Wang, Y., Xiong, W., & Xu, L. (2018). Spatial pattern and temporal stability of root-zone soil moisture during growing season on a larch plantation hillslope in Northwest China. *Forests*, *9*(2), 68. https://doi.org/10.3390/f9020068

Livesley, S. J., Gregory, P. J., & Buresh, R. J. (2004). Competition in tree row agroforestry systems. 3. Soil water distribution and dynamics. *Plant and Soil*, *264*(1–2), 129–139. https://doi.org/10.1023/B:PLSO.0000047750.80654.d5

Ma, J., Liu, X. D., Jin, M., Zhang, X. L., Jing, W. M., Wang, S. L., … Wang, R. X. (2017). Characteristics of rainfall interception by shrubs in Xishui forest district of Qilian Mountains. *Research Soil and Water Conservation*, *24*(3), 363–368 (in Chinese with English abstract).

Majdar, H. A., Vafakhah, M., Sharifikia, M., & Ghorbani, A. (2018). Spatial and temporal variability of soil moisture in relation with topographic and meteorological factors in south of Ardabil Province, Iran. *Environmental Monitoring and Assessment*, *190*(9), 500. https://doi.org/10.1007/s10661-018-6887-9

Malik, R. S., & Sharma, S. K. (1990). Moisture extraction and crop yield as a function of distance from a row of *Eucalyptus tereticornis*. *Agroforestry Systems*, *12*(2), 187–195. https://doi.org/10.1007/BF00123473

Martínez-Fernández, J., & Ceballos, A. (2003). Temporal stability of soil moisture in a large-field experiment in Spain. *Soil Science Society of America Journal*, *67*(6), 1647–1656. https://doi.org/10.2136/sssaj2003.1647

Michel, P., Lee, W. G., During, H. J., & Cornelissen, J. H. (2012). Species traits and their non-additive interactions control the water economy of bryophyte cushions. *Journal of Ecology*, *100*(1), 222–231. https://doi.org/10.1111/j.1365-2745.2011.01898.x

Mishra, A. K., & Singh, V. P. (2010). A review of drought concepts. *Journal of Hydrology*, *391*(1–2), 202–216. https://doi.org/10.1016/j.jhydrol.2010.07.012

Molina, A. J., Llorens, P., Garcia-Estringana, P., de las Heras, M. M., Cayuela, C., Gallart, F., & Latron, J. (2019). Contributions of throughfall, forest and soil characteristics to near-surface soil water-content variability at the plot scale in a mountainous Mediterranean area. *Science of the Total Environment*, *647*, 1421–1432. https://doi.org/10.1016/j.scitotenv.2018.08.020

Nan, G., Wang, N., Jiao, L., Zhu, Y., & Sun, H. (2019). A new exploration for accurately quantifying the effect of afforestation on soil moisture: A case study of artificial *Robinia pseudoacacia* in the Loess Plateau (China). *Forest Ecology and Management*, *433*, 459–466. https://doi.org/10.1016/j.foreco.2018.10.029

Newman, B. D., Wilcox, B. P., Archer, S. R., Breshears, D. D., Dahm, C. N., Duffy, C. J., … Vivoni, E. R. (2006). Ecohydrology of water-limited environments: A scientific vision. *Water Resources Research*, *42*(6), W06302. https://doi.org/10.1029/2005WR004141

Penna, D., Brocca, L., Borga, M., & Dalla Fontana, G. (2013). Soil moisture temporal stability at different depths on two alpine hillslopes during wet and dry periods. *Journal of Hydrology*, *477*, 55–71. https://doi.org/10.1016/j.jhydrol.2012.10.052

Qin, Y., Wu, T., Zhao, L., Wu, X., Li, R., Xie, C., & Liu, G. (2017). Numerical modeling of the active layer thickness and permafrost thermal state across Qinghai-Tibetan Plateau. *Journal of Geophysical Research: Atmospheres*, *122*(21), 11–604. https://doi.org/10.1002/2017JD026858

Raz-Yaseef, N., Rotenberg, E., & Yakir, D. (2010). Effects of spatial variations in soil evaporation caused by tree shading on water flux partitioning in a semi-arid pine forest. *Agricultural and Forest Meteorology*, *150*(3), 454–462. https://doi.org/10.1016/j.agrformet.2010.01.010

Rosecrance, R. C., Brewbaker, J. L., & Fownes, J. (1992). Alley cropping of maize with nine leguminous trees. *Agroforestry Systems*, *17*(2), 159–168. https://doi.org/10.1007/BF00053120

Ruiz-Sinoga, J. D., Galeote, M. G., Murillo, J. M., & Marín, R. G. (2011). Vegetation strategies for soil water consumption along a pluviometric gradient in southern Spain. *Catena*, *84*(1–2), 12–20. https://doi.org/10.1016/j.catena.2010.08.011

Saco, P. M., Willgoose, G. R., & Hancock, G. R. (2007). Eco-geomorphology of banded vegetation patterns in arid and semi-arid regions. *Hydrology and Earth System Sciences Discussions*, *11*(6), 1717–1730.

Seneviratne, S. I., Corti, T., Davin, E. L., Hirschi, M., Jaeger, E. B., Lehner, I., … Teuling, A. J. (2010). Investigating soil moisture–climate interactions in a changing climate: A review. *Earth-Science Reviews*, *99*(3–4), 125–161. https://doi.org/10.1016/j.earscirev.2010.02.004

Shen, Q., Gao, G., Fu, B., & Lü, Y. (2014). Soil water content variations and hydrological relations of the cropland-treebelt-desert land use pattern in an oasis-desert ecotone of the Heihe River basin, China. *Catena*, *123*, 52–61. https://doi.org/10.1016/j.catena.2014.07.002

Shrestha, P., Kurtz, W., Vogel, G., Schulz, J. P., Sulis, M., Hendricks Franssen, H. J., … Simmer, C. (2018). Connection between root zone soil moisture and surface energy flux partitioning using modeling, observations, and data assimilation for a temperate grassland site in Germany. *Journal of Geophysical Research: Biogeosciences*, *123*(9), 2839–2862. https://doi.org/10.1029/2016JG003753

Starkloff, T., Stolte, J., Hessel, R., Ritsema, C., & Jetten, V. (2018). Integrated, spatial distributed modelling of surface runoff and soil erosion during winter and spring. *Catena*, *166*, 147–157. https://doi.org/10.1016/j.catena.2018.04.001

Teuling, A. J., & Troch, P. A. (2005). Improved understanding of soil moisture variability dynamics. *Geophysical Research Letters*, *32*(5), L05404. https://doi.org/10.1029/2004GL021935

Vachaud, G., Passerat de Silans, A., Balabanis, P., & Vauclin, M. (1985). Temporal stability of spatially measured soil water probability density function 1. *Soil Science Society of America Journal*, *49*(4), 822–828. https://doi.org/10.2136/sssaj1985.03615995004900040006x

Valentin, C., d'Herbès, J. M., & Poesen, J. (1999). Soil and water components of banded vegetation patterns. *Catena*, *37*(1–2), 1–24. https://doi.org/10.1016/S0341-8162(99)00053-3

Wang, X., Jiang, Z. R., & Jing, W. M. (2017). Characteristics of frozen soil and freeze-thaw of different vegetation types in Dayekou basin of Qilian Mountains. *Protection Forest Science and Technology*, *3*, 1–4 (in Chinese with English abstract).

Wang, Y., Shao, M. A., Zhu, Y., & Liu, Z. (2011). Impacts of land use and plant characteristics on dried soil layers in different climatic regions on the Loess Plateau of China. *Agricultural and Forest Meteorology*, *151*(4), 437–448. https://doi.org/10.1016/j.agrformet.2010.11.016

Weltzin, J. F., & McPherson, G. R. (1997). Spatial and temporal soil moisture resource partitioning by trees and grasses in a temperate savanna, Arizona, USA. *Oecologia*, *112*(2), 156–164. https://doi.org/10.1007/s004420050295

Western, A. W., Grayson, R. B., Blöschl, G., Willgoose, G. R., & McMahon, T. A. (1999). Observed spatial organization of soil moisture and its relation to terrain indices. *Water Resources Research*, *35*(3), 797–810. https://doi.org/10.1029/1998WR900065

Wilcox, B. P., Breshears, D. D., & Turin, H. J. (2003). Hydraulic conductivity in a pinon-juniper woodland. *Soil Science Society of America Journal*, *67*(4), 1243–1249. https://doi.org/10.2136/sssaj2003.1243

Williams, C. J., McNamara, J. P., & Chandler, D. G. (2009). Controls on the temporal and spatial variability of soil moisture in a mountainous landscape: The signature of snow and complex terrain. *Hydrology and Earth System Sciences*, *13*, 1325–1336. https://doi.org/10.5194/hess-13-1325-2009

Woodall, G. S., & Ward, B. H. (2002). Soil water relations, crop production and root pruning of a belt of trees. *Agricultural Water Management*, *53*(1–3), 153–169. https://doi.org/10.1016/S0378-3774(01)00162-7

Yang, L., Wei, W., Chen, L., Chen, W., & Wang, J. (2014). Response of temporal variation of soil moisture to vegetation restoration in semi-arid Loess Plateau, China. *Catena*, *115*, 123–133. https://doi.org/10.1016/j.catena.2013.12.005

Yu, B., Liu, G., Liu, Q., Wang, X., Feng, J., & Huang, C. (2018). Soil moisture variations at different topographic domains and land use types in the semi-arid Loess Plateau, China. *Catena*, *165*, 125–132. https://doi.org/10.1016/j.catena.2018.01.020

Zhang, P., & Shao, M. A. (2013). Temporal stability of surface soil moisture in a desert area of northwestern China. *Journal of Hydrology*, *505*, 91–101. https://doi.org/10.1016/j.jhydrol.2013.08.045

Zhang, Y., Xiao, Q., & Huang, M. (2016). Temporal stability analysis identifies soil water relations under different land use types in an oasis agroforestry ecosystem. *Geoderma*, *271*, 150–160. https://doi.org/10.1016/j.geoderma.2016.02.023

Zhao, Y., Peth, S., Wang, X. Y., Lin, H., & Horn, R. (2010). Controls of surface soil moisture spatial patterns and their temporal stability in a semi-arid steppe. *Hydrological Processes*, *24*(18), 2507–2519. https://doi.org/10.1002/hyp.7665

Zhu, X., He, Z. B., Du, J., Chen, L. F., Lin, P. F., & Li, J. (2016). Changes in species diversity, aboveground biomass, and distribution characteristics along an afforestation successional gradient in semiarid *picea crassifolia* plantations of northwestern China. *Forest Science*, *63*(1), 17–28. https://doi.org/10.5849/forsci.16-041

Zhu, X., He, Z. B., Du, J., Chen, L. F., Lin, P. F., & Li, J. (2017). Temporal variability in soil moisture after thinning in semi-arid *Picea crassifolia* plantations in northwestern China. *Forest Ecology and Management*, *401*, 273–285. https://doi.org/10.1016/j.foreco.2017.07.022

How to cite this article: Zhu X, He Z, Du J, Chen L, Lin P, Tian Q. Soil moisture temporal stability and spatio-temporal variability about a typical subalpine ecosystem in northwestern China. *Hydrological Processes*. 2020;34:2401–2417. https://doi.org/10.1002/hyp.13737